Self-lubricating PVD Coatings in Interaction with Textured Workpiece Surfaces for Bulk Metal Forming

K. Bobzin[1], T. Brögelmann[1], N. C. Kruppe[1], T.Bergs[2], R. Hild[2], A. Feuerhack[2], D. C. Hoffmann[1*]

[1]Surface Engineering Institute (IOT), RWTH Aachen University, Kackertstr. 15, 52072 Aachen, Germany
[2]Laboratory for Machine Tools and Production Engineering (WZL), RWTH Aachen University, Steinbachstr. 19, 52074 Aachen, Germany

Abstract

Bulk metal forming of steel, in particular forward extrusion, is characterized by high material utilization and resource efficiency. Currently, high quantities of mostly ecologically harmful lubricants are required, leading to the demand for lubricant-free forming. Two approaches are being pursued to achieve the objective of lubricant-free extrusion of steel. One approach focuses on the tool, the other on the workpiece. With regard to the tools, physical vapour deposition (PVD) can be used to apply self-lubricating hard coatings on forming tools. The workpiece-side approach uses texturing of the workpiece surfaces. In this work, one self-lubricating PVD hard coating as well as four different textured workpieces were investigated. The coating was produced in an industrial coating unit. Using a self-designed tool model with the same dimensions as real forming dies with two extrusion shoulders, the coating thickness distribution and the change in coating properties as a function of complex geometry of the forming dies were analysed. Using a pin-on-cylinder tribometer, which represents an open tribological system and simulates the loads of dry bulk metal forming of steel, the interactions between PVD hard coatings and textured workpiece surfaces were investigated. The combination of two approaches of tool coating and workpiece texturing leading to reduction of wear and friction.

Keywords: Physical Vapor Deposition, PVD, Self-lubricating coating, Bulk metal forming, Surface texturing, Open tribological system

1   Introduction

Bulk metal forming is an efficient and resource-saving technology for the mass production of steel components [1] due to high material utilization and achievable degrees of forming as well as low cycle times [2, 3]. These are characterized by good product quality and reproducibility. The high degrees of forming lead to elevated loads within the forming tools, for example contact normal stresses up to $\sigma_N \approx 3{,}000$ GPa [4], resulting in increased tool wear [3, 4]. Therefore, large quantities of lubricants are currently required in order to ensure process reliability. In particular, the use of phosphate-based conversion films and other lubricants that are harmful to the environment and health is widespread in industry [4, 5]. Due to constantly increasing legislative, economic and ecological requirements, there is great interest in enabling a dry forming process through combination of two approaches, with regard to a tool-sided and a workpiece-sided approach.

The application of self-lubricating hard coatings by means of the PVD technology on forming tools represents the tool-side approach to reduce frictional forces between workpieces and tools while at the same time providing wear protection [6, 7]. The self-lubricating properties of these PVD coatings are based on transition metal dichalcogenides, for example molybdenum disulfide [8–10] or tungsten disulfide [11–14], which are widely used as solid lubricants. Transition metal dichalcogenides coatings deposited by PVD technology contribute to a high friction reduction, but cannot withstand the high tribological loads of dry bulk metal forming due to a low indentation hardness $H_{IT} \le 8$ GPa and a weak adhesion to the substrate [15]. Furthermore, transition metal dichalcogenides tend to oxidize in atmosphere [16]. One approach is the combination of transition metal dichalcogenides and a wear-resistant hard coating. Different coating architectures, such as hard-soft combinations, nano-composites, multi- or nanolayer coating architectures, as

well as different elements for the hard phase were investigated [6, 17]. Binary nitride-based coating systems are commonly used for this purpose [18, 19]. Another promising alternative is the ternary coating system (Cr,Al)N with high indentation hardness values up to $H_{IT} = 36$ GPa [20] and promising wear resistance [10, 21].

The workpiece-side solution approach envisages texturing the workpiece surfaces in order to reduce friction and wear through adapted contact conditions between tool and workpiece [22, 23]. A distinction is made between stochastic and deterministic surface texturing. The former are achieved by shot peening and the latter by knurling or laser structuring [24]. The focus of this work lies on the one hand on the analysis of the interaction between self-lubricating PVD hard coatings with various surface textured workpiece, and on the other hand on the investigation of the coating application on complex inner geometries as they are present in forming dies.

2 Experimental procedure

The coating system presented in this paper is based on a hard coating (Cr,Al)N, which has been modified by the incorporation of molybdenum and sulfur. In the following, the coating is referred as (Cr,Al)N+Mo:S. The coating system was deposited with the hybrid technology consisting of direct current magnetron sputtering (dcMS) and high power pulsed magnetron sputtering (HPPMS) in an industrial scale coating unit CC800/9 Custom, CemeCon AG, Wuerselen, Germany, see Figure 1. This has two HPPMS and four dcMS cathodes, which operating simultaneously. Five CrAl20 (chromium base plate with 20 aluminum plugs) and one molybdenum disulfide target were used.
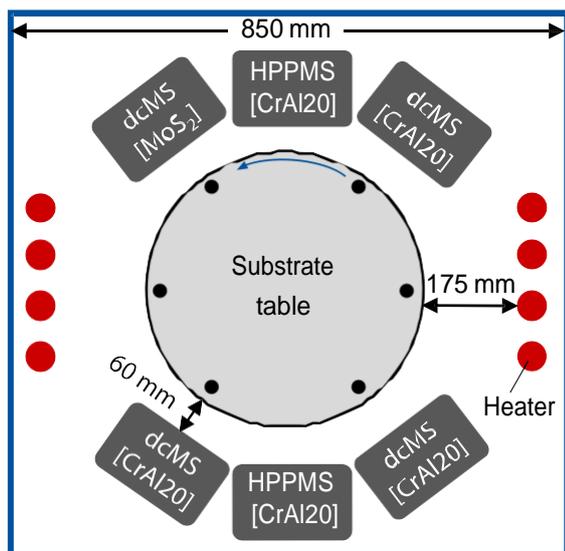

Figure 1: Schematic of the deposition setup

In order to investigate the coating as a function of the complex inner geometry of forming dies, a die model was developed in which five specimens can be attached along this geometry, see Figure 2. The samples P1, P3 and P5

were analyzed at one position ahead (A) and one position behind (B) of the substrate.
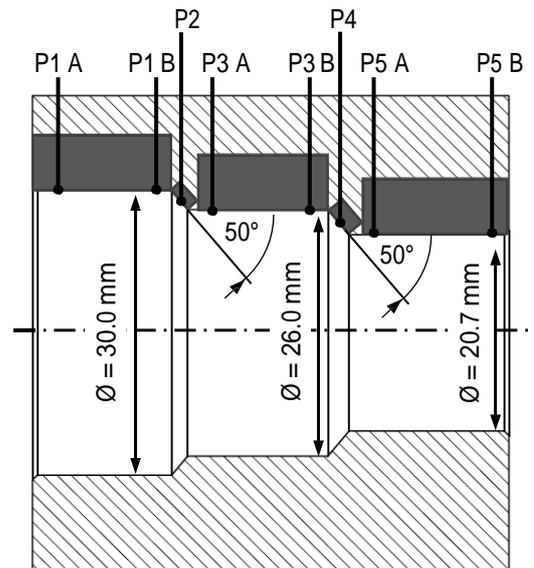

Figure 2: Schematic of the experimental tool with attached AISI M2 substrates and measuring positions P1 A to P5 B

The high-speed steel AISI M2 (DIN 1.3343, HSS 6-5-2) hardened to $H = (60 \pm 1)$ HRC was used as substrate material, since this is typically used for forming tools for bulk metal forming of steel [25]. The process parameters used for coating deposition are illustrated in Table 1.

Table 1: Process parameters for deposition of the coating system (Cr,Al)N+Mo:S

Process parameters	Unit	Value
Max. substrate temperature, T	°C	480
Pressure, p	mPa	710
Argon flux, j(Ar)	sccm	200
Nitrogen flux, j(N$_2$)	sccm	pressure controlled
Power dcMS MoS$_2$, P	kW	2
Power dcMS CrAl20, P	kW	3
Power HPPMS CrAl20, P	kW	5
Pulse frequency, f$_{pulse}$	Hz	500
Pulse length, t$_{on}$	μs	40
Bias voltage, U$_{Bias}$	V	-100

To investigate the coating morphology and thickness, cross-sectional micrographs were analyzed using a scanning electron microscope (SEM), ZEISS DSM 982 Gemini, Carl Zeiss AG, Oberkochen. The chemical composition was analyzed by means of an electron probe microanalyser (EPMA), Schottky emitter electron microprobe, JEOL JXA8530F, Tokyo, Japan. Both investigations have been carried out at the Central Facility for Electron Microscopy (GFE) of the RWTH Aachen University. The mechanical properties were

determined using nanoindentations with a Berkovich indenter. A nanoindenter of the type TI 950, Bruker Corporation, Billerica, Massachusetts, USA, was used for this investigation. The indentation depth was less than 10 % of the coating thickness. The calculation of the indentation modulus is based on the equations of Oliver and Pharr [26], whereby a constant Poisson's ratio of $v = 0.25$ was assumed for the coatings. SEM, energy dispersive X-ray spectroscopy (EDS) and confocal laser scanning microscopy (CLSM) Keyence VK X210, Tokyo, Japan, were used for wear analysis. A pin-on-cylinder (PoC) tribometer was used to simulate the stress collective occurring in bulk metal forming of steel, see Figure 3.
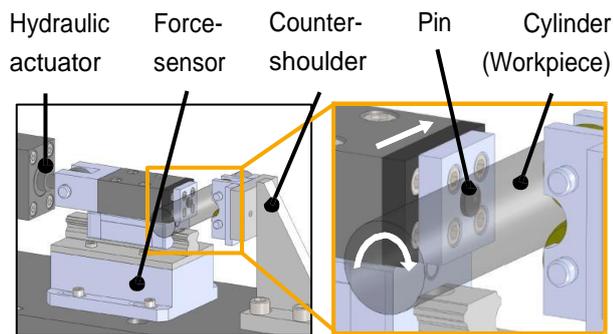

Figure 3: Schematic of the experimental setup of the pin-on-cylinder tribometer

The boundary conditions are listed in Table 2. Additionally, the workpiece and tool materials, which are commonly used in forward extrusion, are also depicted in Table 2.

Table 1: Boundary conditions of the pin-on-cylinder tests

	Standard/ Unit	Designation/ Value
Pin material	AISI	M2
Workpiece material	AISI	5115
Normal force F_N	N	2,600
Rounds per minute rpm	1/min	19
Feed rate	mm	8
Pin radius r_{Pin}	mm	15

At the pin-on-cylinder test, cylinders with three different textured cylinder surfaces and one grinded cylinder surface as reference were tested to investigate the influence on the tribological behavior. They were shot peened with ceramic-mix beads, steel beads and sharp-edged corundum, respectively. The shot peening parameters are shown in Table 3.

Table 2: Shot peening parameters

	Particle form	Particle size [µm]	Particle density [g/cm³]	Particle hardness [HV]	Peening pressure [bar]
Ceramic-mix	round	125-250	3.8	1,200	2
Steel	round	700-1,000	7.8	390-535	3
Corundum	sharp	425-600	3.9-4.1	2,600	4
Reference	-	-	-	-	-

The ceramic-mix beads consist of $x_{ZrO2} = 62$ wt.-% zirconiumdioxide, $x_{SiO2} = 28$ wt.-% silicondioxide, $x_{Al2O3} = 5$ wt.-% aluminum oxide and small amounts of calcium, iron and titanium oxides. A list of the resulting surface properties of the cylinders after the shot peening process are listed in Table 4.

Table 3: Cylinder hardness and roughness after shot peening

	Cylinder hardness and roughness		
	HV1 [HV]	Sa [µm]	Sz [µm]
Ceramic-mix	410	1.15	24.58
Steel	280	2.82	31.96
Corundum	260	3.78	57.02
Reference	200	0.43	4.36

The highest surface near hardness exhibits the cylinder shot peened by ceramic-mix peening media. Cylinders shot peened by corundum have the highest roughness.

3 Results and discussion

In order to provide a better overview of the current results, the in [7] published results of the coating characterization can be seen in Figure 4 and Table 5. For investigation of the coating topography and morphology of coated substrates, which were orientated parallel to the targets, micrographs were taken using a secondary electrons (SE) detector in a SEM, see Figure 4The coating (Cr,Al)N+Mo:S was deposited on the substrate material AISI M2. In order to ensure a good adhesion to the substrate, a metallic bondcoat (Cr,Al) and a nitridic interlayer (Cr,Al)N were deposited before the toplayer (Cr,Al)N+Mo:S.
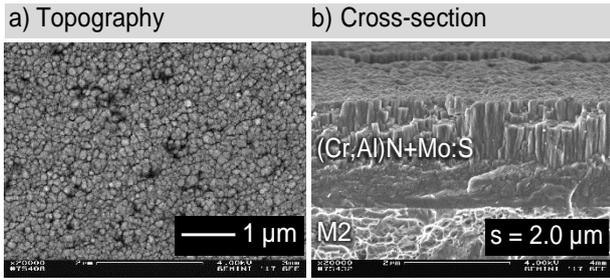
a) Topography   b) Cross-section

Figure 4:   SEM micrographs of the surface topography (a) and cross-section (b) of the coating system (Cr,Al)N+Mo:S [7]

The coating exhibit a smooth, cauliflower-like surface topography with an arithmetic surface roughness of Sa = 0.03 µm. Furthermore, it reveals a fine columnar microstructure and a coatings thickness of s = 2.0 µm. The chemical composition was analyzed using EPMA and the mechanical properties were determined by means of nanoindentation with a constant load of F_N = 10 mN, see Table 5.

Table 4:   Chemical composition and mechanical properties of the coating system (Cr,Al)N+Mo:S [7]

	Chemical composition [at.-%]					Mechanical properties [GPa]	
	Cr	Al	N	Mo	S	H_{IT}	E_{IT}
(Cr,Al)N +Mo:S	37.9	4.6	50.3	4.5	2.8	21.0 ± 2.1	280.6 ± 29.2

To evaluate the tribological behavior of the (Cr,Al)N+Mo:S coatings at a load collective similar to that of full forward extrusion, PoC tests without lubricants were performed with uncoated pins as reference and coated pins. In addition, various cylinders or semi-finished products of material AISI 5115, mechanically pretreated by shot peening with different shot media, were used as counter bodies. The apparent coefficient of friction CoF*, which is calculated from the ratio of normal force F_N to tangential friction force, see Figure 5, is applied because the high normal forces lead to a plastic deformation of the cylinder.

Overall, it can be stated that all tested coated pins led to a significant friction reduction compared to the uncoated pins. Furthermore, the apparent coefficient of friction CoF* of the coated pins remain at a constantly low level with CoF* ≈ 0.2 - 0.3, whereas the apparent coefficient of friction CoF* of the uncoated pins initially increase rapidly and then decrease slowly. Additionally, it can be seen that the different surface finishes of the cylinders have a small influence on the apparent coefficient of friction CoF* of the coated pins, but a considerable influence on the uncoated pins. With regard to the friction, the most promising combination is a cylinder pre-treated with steel beads and a coated pin.

The wear analyses of the uncoated pins were carried out by CLSM in order to see the respective surfaces of the pins as well as 3D-micrographs, see Figure 6. The curvature of the pin contours was corrected by software in order to flatten it and to improve the visibility of the 3D-images. The arrow indicates the relative movement of the pins.

The main wear mechanism is the adhesion of the soft cylinder material AISI 5115 to the pins. During the PoC tests with uncoated pins, a continuous build-up and tear-off of the cold welds could be observed, which explains the fluctuating course of the apparent coefficient of friction. The analysis of the wear of the coated pins was carried out using SEM and CLSM 3D-micrographs, see Figure 7. To assess whether adhesive or abrasive wear is present, additional EDS point measurements were carried out, see Table 6. The pins coated with (Cr,Al)N+Mo:S have significantly improved wear resistance compared to the uncoated pins. Especially those that were tested against the cylinders shot peened with ceramic-mix and steel beads.
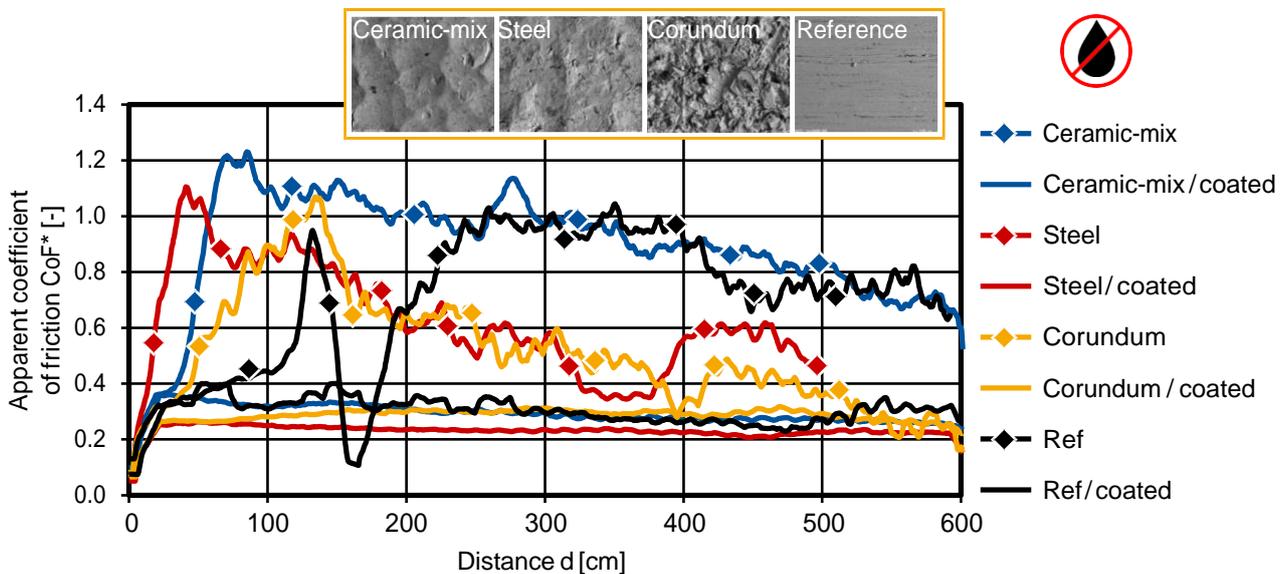

Figure 5:   Apparent coefficient of friction CoF* of uncoated and coated pins of AISI M2 tested against cylinders of AISI 5115 with different surface topographies
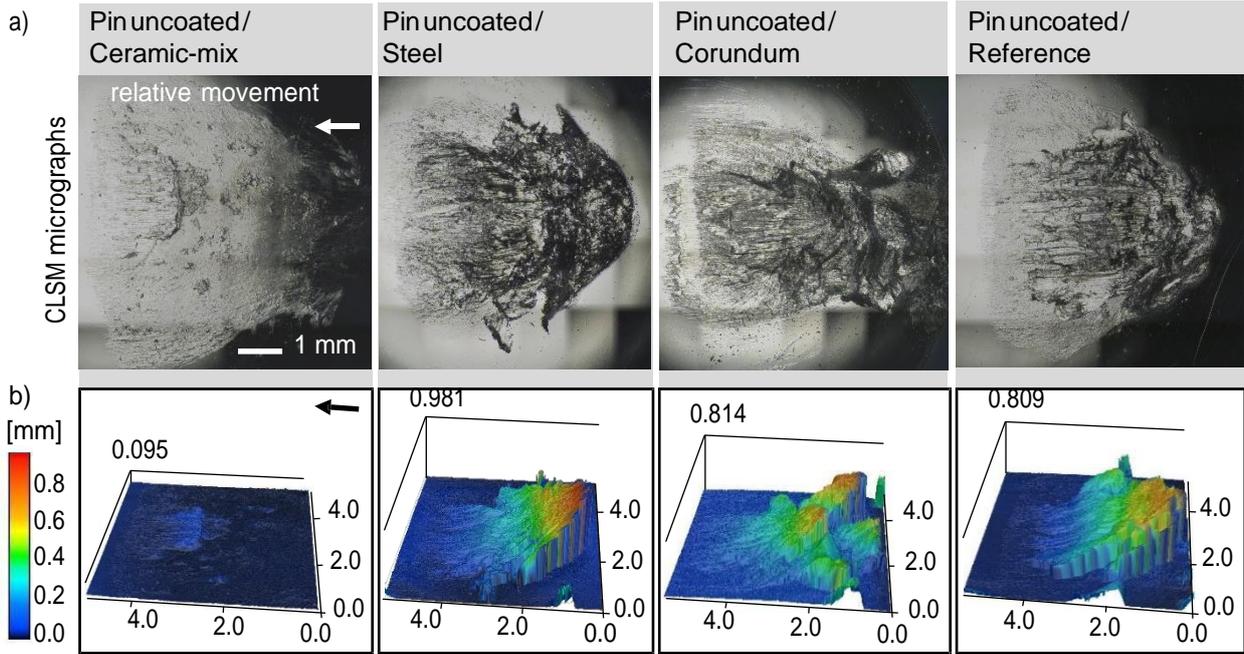
Figure 6: CLSM images (a) and 3D-micrographs (b) of the uncoated pins after pin-on-cylinder test

The EDS measurements, Ceramic-mix P1 and P2 as well as Steel P1 reveal that these coatings exhibit only very small areas with slight adhesive wear. Only the combination pin coated / Corundum is partly delaminated at P3, which is evident by the substrate materials vanadium and tungsten, which results in adhesive wear. This can be explained by the sharp-edged topography of the Corundum-shot peened surface. The wear volume of the combination pin coated / Steel is $W_V = 5.4 \cdot 10^9$ µm³, whereas the combination pin uncoated / Steel is $x = 630$ times higher with $W_V = 3,448.5 \cdot 10^9$ µm³. In addition, small adhesive cold weldings could be observed with pin coated / Reference, see Reference P2, which is probably due to the changed contact conditions due to the relatively smooth cylinder surface. Overall, the combination of self-lubricating

coating and textured cylinder surface pin coated / Steel exhibits the highest potential for the realization of lubricant-free bulk metal forming of steel.

In order to verify whether the coating process is suitable for a successful coating deposition on complex inner geometries of forming dies with high aspect ratios, the die model described in Figure 2 was used. To determine the coating thickness distribution and to analyses the coating morphology, SEM cross-sectional micrographs of the five samples were taken at the measuring points P1 A to P5 B, see Figure 8. A consistent, area-wide and dense coating formation from the beginning to the end of the tool can be seen. This is not necessarily the case due to the strong line of sight characteristics of PVD processes. The SEM cross-sectional micrographs reveal that the dcMS/ HPPMS
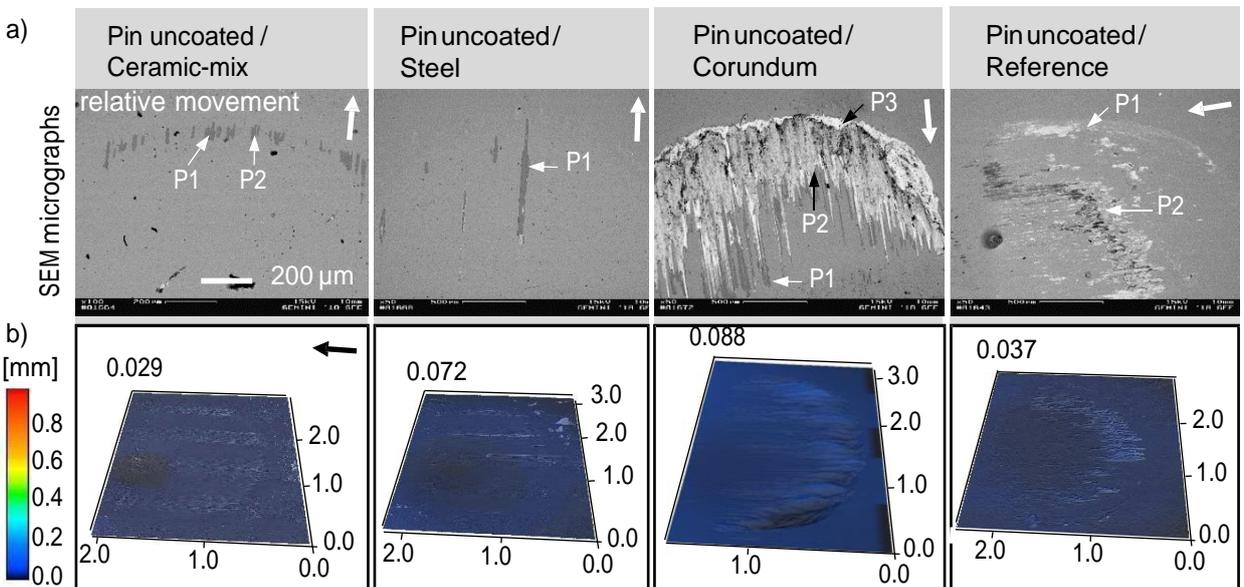

Figure 7: CLSM images (a) and confocal laser scanning microscopy 3D-micrographs (b) of the uncoated pins tested by pin-on-cylinder tribometer

technology enables the deposition of a continuous and dense coating on a complex interior geometry with an aspect ratio of AR > 2 of a forming die with two extrusion shoulders.

Table 5: EDS point measurements of the coated pins after pin-on-cylinder tests

Pins coated vs.	Ceramic-mix		Steel	Corundum			Reference	
Position	P1	P2	P1	P1	P2	P3	P1	P2
Cr [at.-%]	74.5	73.7	74.8	73.1	1.3	4.9	64.1	3.1
Al [at.-%]	19.1	19.6	19.3	18.3	6.1	1.0	8.0	3.6
Mo [at.-%]	1.3	0.50	1.0	0.6	-	5.1	9.3	0.7
Fe [at.-%]	5.1	6.2	4.9	8.0	92.6	72.8	18.6	92.7
V+ W [at.-%]	-	-	-	-	-	16.2	-	-

The coating thickness decreases as a function of the bore depth. However, the extrusion shoulders at positions P2 and P4 are less affected, as these exhibit direct lines of sight to the targets due to the shoulder opening angle of α = 50 °. As samples P2 and P4 are also continuously shadowed by the targets due to rotation, the respective deposition rates are lower than for flat, unshaded substrates.

The coating thickness decreases from s = 2.3 µm to s = 1.0 µm from the beginning of the inlet area to the first extrusion shoulder by more than Δs = -50 %. With greater bore depths, the coating thickness of P5 A and P5 B is reduced to s = 0.4 µm. When looking at the coating morphologies, it can be seen that, except for the extrusion shoulders P2 and P4 which exhibit a dense, fine crystalline microstructure, a fine columnar microstructure has formed throughout. The column boundaries of samples P1 and P3 are not aligned orthogonally to the substrate as usual, because the borehole of the die to be coated is aligned by β = 90° to the targets. However, the specimen P5 B reveals that the alignment of the columns has changed due to a coating deposition from the rear borehole. In addition, the coating topography is very smooth throughout.
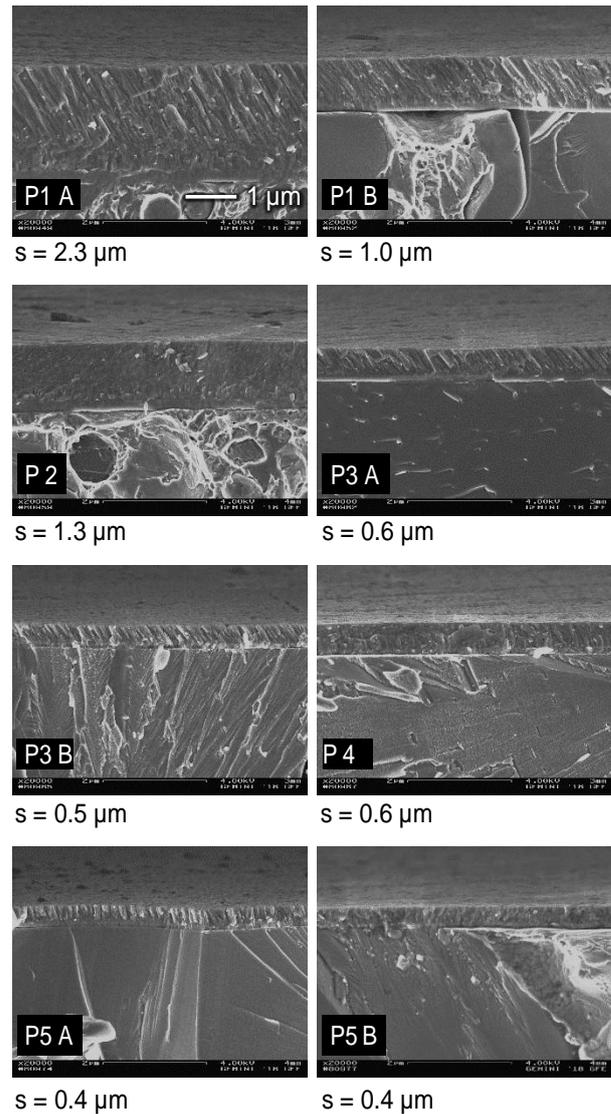

Figure 8: SEM cross-sectional micrographs of the (Cr,Al)N+Mo:S coated AISI M2 substrates at positions P1 A to P5 B along the bore depth of the die

4 Conclusion

The tribological investigations using the pin-on-cylinder test and subsequent wear analyses reveal the self-lubricating properties and wear resistance of the (Cr,Al)N+Mo:S coating system. The combination of this PVD tool coating and semi-finished products pre-treated with ceramic-mix shot media exhibits the highest potential for dry bulk metal forming of steel. A successful application of the self-lubricating hard coating (Cr,Al)N+Mo:S on the high-speed steel AISI M2 by means of the hybrid technology dcMS/ HPPMS on complex inner geometries with high aspect ratios was shown with the help of the die model as well as SEM cross-sectional micrographs. The investigations show the high potential of the dcMS/ HPPMS technology for the application of friction-reducing and wear-resistant tool coatings on reducing dies for bulk metal forming of steel.

References

[1] T. Herlan, Optimaler Energieeinsatz bei der Fertigung durch Massivumformung, Berichte aus dem Institut für Umformtechnik der Universität Stuttgart 1991.

[2] F. Klocke, Manufacturing Processes 4, Springer Berlin Heidelberg, Berlin, Heidelberg 2013.

[3] K. Lange, Fliesspressen: Wirtschaftliche Fertigung metallischer Präzisionswerkstücke, Springer, Berlin 2008.

[4] N. Bay, A. Azushima, P. Groche, I. Ishibashi, M. Merklein, M. Morishita, T. Nakamura, S. Schmid, M. Yoshida, CIRP Ann., 2010, 59, 760.

[5] T. Mang, W. Dresel, Lubricants and lubrications, Wiley-VCH, Weinheim, 2007.

[6] J.-F. Yang, B. Parakash, J. Hardell, Q.-F. Fang, Front. Mater. Sci., 2012, 6, 116.

[7] K. Bobzin, T. Brögelmann, N.C. Kruppe, D.C. Hoffmann, F. Klocke, P. Mattfeld, D. Trauth, R. Hild, Surf. Coat. Technol., 2018, 353, 282.

[8] X. Zhang, W. Lauwerens, L. Stals, J. He, J.-P. Celis, J. Mater. Res., 2001, 16, 3567.

[9] D.G. Teer, J. Hampshire, V. Fox, V. Bellido-Gonzalez, Surf. Coat. Technol., 1997, 94-95, 572.

[10] K. Bobzin, T. Brögelmann, N.C. Kruppe, S. Basturk, F. Klocke, P. Mattfeld, D. Trauth, R. Hild, Surf. Coat. Technol., 2016, 308, 383.

[11] K. Bobzin, T. Brögelmann, N.C. Kruppe, M. Arghavani, S. Bastürk, F. Klocke, P. Mattfeld, D. Trauth, R. Hild, Dry Met. Forming OAJ FMT, 2016, 2, 72.

[12] B. Deepthi, H.C. Barshilia, K.S. Rajam, M.S. Konchady, D.M. Pai, J. Sankar, A.V. Kvit, Surf. Coat. Technol., 2010, 205, 565.

[13] L. Lind, E. Adoberg, L. Aarik, P. Kulu, R. Veinthal, A.A. Aal, Estonian J. Eng., 2012, 18, 193.

[14] T.W. Scharf, A. Rajendran, R. Banerjee, F. Sequeda, Thin Solid Films, 2009, 517, 5666.

[15] A. Aubert, J.P. Nabot, J. Ernoult, P. Renaux, Surf. Coat. Technol., 1990, 127.

[16] P. Voumard, A. Savan, E. Pflüger, Lubr. Sci., 2001, 13, 135.

[17] S. Carrera, O. Salas, J.J. Moore, A. Woolverton, E. Sutter, Surf. Coat. Technol., 2003, 167, 25.

[18] Y. LI, S. KIM, Rare Met., 2006, 25, 326.

[19] A. Nossa, A. Cavaleiro, Surf. Coat. Technol, 2003, 163-164, 552.

[20] B. Tlili, N. Mustapha, C. Nouveau, Y. Benlatreche, G. Guillemot, M. Lambertin, Vacuum, 2010, 84, 1067.

[21] K. Bobzin, T. Brögelmann, N.C. Kruppe, M. Arghavani, Adv. Eng. Mater., 2017, 19, 1600632.

[22] R. Hild, A. Feuerhack, D. Trauth, D.C. Hoffmann, N.C. Kruppe, T. Brögelmann, K. Bobzin, F. Klocke, MATEC Web Conf., 2018, 190, 14009.

[23] P. Groche, J. Stahlmann, J. Hartel, M. Köhler, Trib. Int., 2009, 42, 1173–1179.

[24] D. Trauth, R. Hild, P. Mattfeld, S. Bastürk, T. Brögelmann, K. Bobzin, F. Klocke, Proceedings of the 12th International Conference THE „A" Coatings in Manufacturing Engineering, Hannover, Germany, March 31th - April 1st, 2016, 185.

[25] A. Hettig, Einflußgrößen auf den Werkzeugbruch beim Voll-Vorwärts-Fließpressen, Berichte aus dem Institut für Umformtechnik der Universität Stuttgart 106, 1990.

[26] W.C. Oliver, G.M. Pharr, J. Mater. Res., 1992, 7, 1564.

[27] K.-H. Grote, E.K. Antonsson (Eds.), Springer handbook of mechanical engineering, Springer-Verlag, Berlin, Heidelberg 2009.

[28] R. Hild, A. Feuerhack, D. Trauth, M. Arghavani, N. Kruppe, T. Brögelmann, K. Bobzin, F. Klocke, Proceedings of the 13th International Conference THE „A" Coatings in Manufacturing Engineering, Thessaloniki, Greece, October 5th - 6th, 2017, 103.